49th European Rotorcraft Forum, 5-7 September 2023, Bückeburg, Germany
https://publikationen.dglr.de/?id=620&tx_dglrpublications_pi1[document_id]=54801000

PERFORMANCE, ENVIRONMENTAL, AND MOBILITY ANALYSIS OF LARGE CAPACITY FAST ROTORCRAFT CONFIGURATIONS FOR THE EUROPEAN REGIONAL AIR TRAFFIC MARKET

M.Sc., Laurent Declerck, Royal Netherlands Aerospace Centre, The Netherlands
M.Sc., Marc Cruellas Bordes, Royal Netherlands Aerospace Centre, The Netherlands
M.Sc., Ph.D., Chana Anna Saias, Cranfield University, United-Kingdom
M.Sc., Ph.D., Devaiah Nalianda, Cranfield University, United-Kingdom
M.Sc., Ph.D., B. Deneys J. Schreiner, Cranfield University, United Kingdom
M.Sc., Ph.D., Gianluigi A. Misté, University of Padova, Italy
M.Sc., Ph.D., Andrea Dal Monte, University of Padova, Italy
Prof. Ernesto Benini, University of Padova, Italy
Alf Junior, German Aerospace Centre, Germany

Abstract

Fast, large rotorcraft are of interest in the future European air transport system due to their runway independent operation and potential mobility improvements for the passenger. Both a tiltrotor and a coaxial compound concept model were developed for a 70 passenger, 500 NM design mission that would compete with regional fixed-wing aircraft. These models were flown along virtual trajectories representing possible use-cases and assessed for environmental performance in comparison to an in-service baseline aircraft using comparable engine technology levels. Further, the travel time and mobility improvement available to the intermodal transport network through the inclusion of these concept rotorcraft was examined with promising results. Future work is suggested to address the shortfall in environmental performance.

1. NOTATION

Symbols

c_l, c_d, c_m	Aerodynamic coefficients, -
C_T	Thrust coefficient, -
D	Drag, N
M	Mach number, -
V_{br}	Velocity best range, kts
V_e	Velocity best endurance, kts
η_{poly}	Polytropic efficiencies, -
σ	Solidity, -

Acronyms:

CRP	Contingency Rated Power
EMMA	European Multi-Modal Analysis
EW	Empty Weight
EWF	Empty Weight Fraction
FLC	Fast Large Compound
FLT	Fast Large Tiltrotor
FRC	Fast Rotorcraft Concept
GSP	Gas turbine Simulation Program
HOGE	Hover Out of Ground Effect
MCP	Maximum Continuous Power
MRP	Maximum Rated Power
MTOW	Maximum Take Off Weight
NUTS	Nomenclature of Territorial Units for Statistics
OEI	One Engine Inoperative
OEW	Operational Empty Weight
PR4	Population reached in ≤ 4 hours
SRIA	Strategic Research & Innovation
VTOL	Vertical Take Off and Landing

2. INTRODUCTION

2.1. Background

Strategic Research & Innovation Agenda (SRIA) goals have been set for the European aviation industry to ensure future environmental sustainability while meeting society's needs for fast and efficient transportation. Fast rotorcraft are seen as a potential enabling technology in achieving these ambitious goals.

This paper will present and discuss a part of the results of the project FASTRIP2050 (FAST Rotorcraft Societal Integration and Performance Assessments 2050). This project investigates the performance, environmental impact, and mobility benefits of fast large capacity tiltrotor aircraft and compound rotorcraft configurations. FASTRIP2050 is part of the European Clean Sky 2 project and falls under the Technology Evaluator, which is an evaluation platform to assess the environmental impact and societal benefits of cutting-edge aviation technologies. The project consortium includes the Royal Netherlands Aerospace Centre (NLR), ANOTEC Engineering, the University of Padova and is led by Cranfield University.

2.2. Motivation

The motivation for this project is the evident increasing need for fast, efficient, and environmentally friendly transportation. The potential benefits and impact of introducing Fast Rotorcraft Concepts (FRCs) is studied in this research. Limitations on future air transport provision may still arise even if ground transportation networks are able to increase capacity to match the predicted growth. This leads to Vertical Take-Off and Landing (VTOL) aircraft becoming a more attractive technology as the utilisation of smaller airports or optimally located heliports may be exploited.

The introduction of large-capacity FRCs in commercial fleets would target reductions in congestion at both airport and ground transport level. This becomes possible by permitting some short-haul traffic to shift to rotorcraft, thereby relieving runway and terminal area congestion and increasing free runways for larger aircraft. From the study in Ref. 1, it was concluded that approximately 10% of commercial flights in 2017 could be performed by Runway Independent Aircraft (RIA), which projects a reduction in total delay duration for the remaining flights of 79%. The prime markets could be point-to-point trips (both intra- and intercity) and commuter connections to congested hub airports. Additionally, the utilisation of large-capacity rotorcraft can free up slots in busy airports as these configurations are foreseen to operate like short-range commuter aircraft from airport hub feeders in small cities to congested or slot-constrained hub airports.

Commuter turboprop aircraft are currently the main operators of these services and are thus the appropriate reference technology for the large-capacity FRCs. The prime markets for FRC operations could be high density intercity passenger and airport feeder services in the busiest air corridors. Benefits to passengers may be attained due to improved mobility and reductions in overall travel time. This time saving hinges on well-situated heliports: since rotorcraft do not need long runways, two hectares or smaller heliports (Ref. 2) might be built at accessible locations where conventional airports are unfeasible or prohibitively expensive. Additionally, heliports co-located with existing airports could permit increased flights to the airport without clogging runways. Commercial rotorcraft operations from urban heliports or airports will necessarily require new ground facilities, air traffic control equipment, and procedures for terminal airspace. In contrast to these benefits, cost and noise are significant considerations in the feasibility of those concepts as civil aviation and regulatory policies and the rotorcraft will be subject to the same constraints.

3. ROTORCRAFT DEFINITION

3.1. Mission Scenario

A design mission is defined and selected to compare the large-capacity rotorcraft with the reference technology, the ATR72-600. The design mission specifications are presented in Table 1. The short-haul regional market is foreseen to be targeted for the investigated large rotorcraft. A design range of 500 NM is used to size the large FRC. This was selected based on 2015 fleet data as mission ranges up to 500 NM are responsible for 40% of the total aircraft departures globally (Figure 1) Ref. 3, the ATR72-600 reference aircraft operates at ranges below 500 NM for most of its missions. The selected payload is set to 70 passengers (pax) to be comparable with the ATR72-600, which is designed to carry 72.

Table 1: Design mission FRC

Design Mission
3 min taxi, 5k ft ISA +20˚C
2 min HOGE, 5k ft ISA +20˚C (95% MCP)
Climb at maximum climb rate, best climb speed
Cruise at best range velocity (V_{br}) for 500 NM

Descend at V_{br} (no range credit) (~1500 ft/min)
1 min HOGE, 5k ft ISA +20˚C
Reserve (alternate airport): 100 NM V_{br}
Reserve (emergency): 30 min V_e, 5k ft ISA
Design Power - Engine Requirements
Hover: MRP, 5k ft ISA+20˚C
Cruise: MCP V_{br}, ISA+20˚C
OEI hover CRP, 5k ft ISA+25˚C

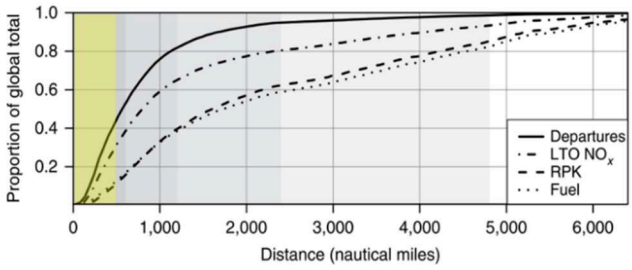

Figure 1: Cumulative distributions of key operational variables by global commercial aircraft fleet in 2015 adapted from Ref. 3

3.2. Rotorcraft sizing

Fast Large Tiltrotor (FLT)

The MTOW of the tiltrotor was set using statistical relations found from studying other civil tiltrotor reference aircraft and concept studies, Ref. 4, 5, 6, 7 and 8. A high-level mass breakdown of the aircraft was estimated using statistical data (EW, payload, mission fuel). The empty weight fraction (EWF) was set to 0.65 for the large capacity tiltrotor with an EW of 22 773 kg and a MTOW of 34 930 kg. The maximum fuel capacity volumetric constraint was set to 5 000 kg of fuel, matching the reference aircraft (ATR 72-600). The FLT features a cross-shaft which limits the available volume in the wings for fuel storage. When compared to the ATR 72-600, it is assumed that the larger wing area and higher thickness to chord (t/c) ratio of the FLT compensates for the volume loss due to the cross-shaft and justifies a 5 000 kg fuel capacity.

The rotor disk loading was set 74 kg/m^2 based on data from reference civil tiltrotors such as the NASA concept study Ref. 8. The rotor RPM is scheduled based on the aircraft flight mode. The maximum tip speed was set to M = 0.64, a trade-off between blade loading, auto rotation performance, acoustic signature, and power. A maximum blade loading of C_T/σ = 0.17 was set for the worst-case condition of the design mission at 5k ft ISA+20°C in hover to allow for enough margin for gust tolerance and manoeuvres.

The main wing loading was set to 508 kg/m^2 based on data interpolation using design parameters from reference civil tiltrotors. A wing taper ratio of 1 was assumed between the fuselage and the nacelles for structural reasons. A taper ratio of 0.6 was set for the wing tips outboard of the rotor nacelles. Flaperons are positioned over the span section of the wing between the nacelles.

The fuselage aerodynamic coefficients lookup table was scaled from XV15 data to match the correct value for the FLT fuselage cross section. The FLT aircraft features four 3 560 kW engines. Current engine technology is assumed. The OEI low-speed situation in hot and high conditions (5k ft ISA+20°C) is found to be the dominant sizing condition for the engines. At the OEI situation, the engine is operating at the contingency power rating (CPR) which is 1.33 times the max continuous power (CRP = 1.33 MCP).

Fast Large Compound (FLC) rotorcraft

A generic coaxial compound rotorcraft comprising a stiff counter-rotating coaxial system and a pusher propeller (modelled after the Sikorsky X2TD Ref. 9, 10) was selected as the baseline to model the large-capacity architecture. The configuration has been developed and validated in previous studies Ref. 11.

This architecture has been selected for the large capacity investigation as it offers several advantages: achieving high-speed cruise and removal of the tail rotor requirement. However, the edgewise rotors are not sufficient to generate the propulsive thrust required at high speed and thus a tail-mounted propeller is utilised.

The FLC configuration is sized for the same design mission (Table 1). The sizing and design of this concept were verified against the Sikorsky RVR data (Figure 2) Ref. 32. The fuselage is first sized for a 70-passenger arrangement with a total length of 30 m. The fuselage is assumed to be streamlined resulting in lower drag compared to conventional helicopters in order to be comparable with fixed-wing regional aircraft. The aerodynamic coefficients of lift (c_l), drag (c_d), and pitching moment (c_m) are expressed as a function of incidence angle based on fuselage data of the Bell XV-15. Similarly, the empennage is represented using look-up tables based on the Bell XV-15 Ref. 12.

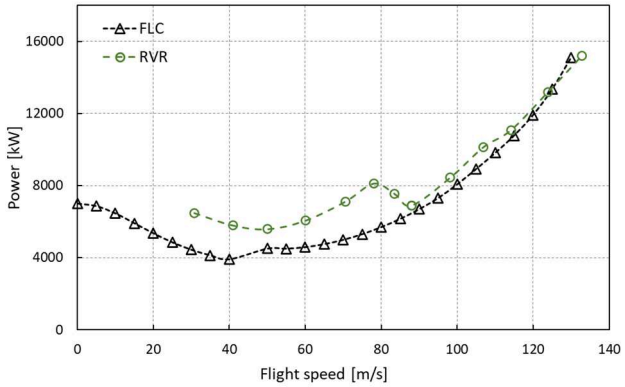

Figure 2: Total power requirement for compound rotorcraft as a function of flight speed at SL conditions

A zero-incidence flat plate area is selected based on historical trends (Ref. 13, 14) assuming airframe drag to dynamic pressure ratio D/q = 0.149 m^2 for future conceptual airframes. For the rotor hub drag, a coefficient of C_D = 0.0015 represents faired hubs is selected Ref. 11. The fuselage, rotor hubs, rotor shafts, and empennage contribute to the total airframe drag. The horizontal stabiliser is used to offload the main rotors in the cruise segment.

The specifications of the FLC rotorcraft are summarised in Table 2. Once the top-level aircraft requirements and mission is defined, the maximum take-off weight (MTOW) is estimated using correlations derived from statistical data from the open literature. The MTOW is calculated at 43 000 kg and an empty weight (EW) fraction of 70% is assumed as per Ref. 7. A high-level mass breakdown of the aircraft was also estimated using statistical data (EW, payload, mission fuel). The maximum fuel capacity is set to 5000 kg.

The main rotor geometry is modelled after the Sikorsky X2TD. At hover, the main rotor rotational speed in revolutions per minute (RPM) is set based on the assumed maximum blade tip speed of 190 m/s. The main rotors' speed is reduced during high-speed flight by limiting the advancing blade tip Mach number to M < 0.9 Ref. 11. The rotor radius is evaluated using a disk loading of 73.2 kg/m^2 based on the conceptual compound rotorcraft in Ref. 15. The pusher propeller is connected via a clutch so that it may be engaged at high forward speeds and disengaged at low forward speeds. During low-speed flights, the propeller is autorotating to minimise drag. The resulting propeller drag is low compared to the rest of the airframe and is thus omitted. The RPM of the propeller is set using a tip speed of 280 m/s at high-speed cruise conditions.

Standard coaxial helicopter controls plus aircraft pitch and roll attitude are used in hover and low-speed flight to trim the FLC. The propeller is engaged for forward speeds above 50 m/s where the main rotors are slowed to comply with the tip Mach number limits. At these speeds, the pitch angle is prescribed to 1.6° nose-up attitude and the propeller collective pitch is trimmed instead. Below this speed, the fuselage attitude is a determined trim parameter.

The propulsion system is sized with respect to predefined power ratings as elaborated in Ref. 16. Atmospheric conditions are taken using the international standard atmosphere (ISA):

- Hover: 95% maximum rated power (MRP), 5k ft ISA+20˚C;
- Cruise: 100% maximum continuous power (MCP) at best altitude;
- One engine inoperative (OEI): for take-off at 5k ft ISA+20˚C the contingency power of the remaining engines (assessed at 133% OEI MCP) must be greater than 90% of hover out of ground-effect (HOGE) power.

The FLC is powered by three current technology level kerosene-fuelled turboshaft engines. The component polytropic efficiencies (η_{poly}) used are adapted based on Ref. 17. The engine is sized at the MCP rating, which acts as the design point. The NOx modelling method used for the FLT is also used for the FLC.

Table 2: Fast Rotorcraft specifications

Parameter	FLC	FLT
MTOW	43 000 kg	34 930 kg
EW	30 000 kg	22 773 kg
Payload (70 pax)	7350 kg	7350 kg
EWF	0.70	0.65
Fuel tank capacity	5000 kg	5000 kg
Fuselage		
Fuselage length	30 m	27.16 m
Fuselage width	3.4 m	2.75 m
Main Rotors		
Rotor radius	12.5 m	8.67 m
Number of blades	2 x 4	2 x 4
Disk loading (@ MTOW)	73.2 kg/m^2	74 kg/m^2
Rotor speed hover	139 RPM	228 RPM
Main Wing		

Wing loading (@ MTOW)	-	506 kg/m2
Overall wing span	-	27.42 m
Propeller		
Rotor radius	4.2 m	-
Number of blades	6	-
Propeller speed	66.2 rad/s	-
Gas turbine engines		
Engine number	3	4
MCP per engine	4000 kW	3560 kW

3.3. Reference Aircraft

The reference aircraft selected to be compared with the FASTRIP FRCs is a regional aircraft modelled on the ATR 72-600. This configuration is powered by two PW127N turboprops, Ref. 18, 19. The basic design data is presented in Table 3, Ref. 18. The baseline aircraft is designed to accommodate 72 passengers based on the 29" pitch ATR 72-600.

Table 3: Reference aircraft specifications Ref. 18, 19

Parameter	Value
OEW	13 310 kg
Ramp weight	22 968 kg
Payload	7 409 kg
Max fuel capacity	5000 kg
Wing area	61.0 m^2
Wing loading at take-off	376.53 kg/m^2

4. METHODOLOGY

4.1. Simulation model tiltrotor FLT

FLIGHTLAB is used for the performance modelling of the large capacity tiltrotor. The large capacity tiltrotor FLIGHTLAB model features two gimballed four-bladed rotors with hinged rigid blades. A blade element model is used to predict rotor performance. A 3-state Peters-He inflow model is used to calculate the induced velocity through the rotor. The rotor RPM and nacelle tilt angle are determined from flight speed according to a predefined schedule. The engine nacelles are modelled by aerodynamic forces and moments lookup tables.

The main wing is simulated by a 3D lifting line model which is combined with nonlinear lookup tables to provide the wing aerodynamic coefficients. A semi-empirical method is used to compute the downwash effect of the rotors on the wing, Ref. 20, 21. The trailing edge wing flaps are deflected downwards during slow speed flight to reduce the download effect.

A control architecture is defined to fly the FLT in both slow speed 'helicopter mode' and cruising, high speed 'airplane mode'. In helicopter mode, the rotor (symmetric) collective and (symmetric) longitudinal cyclic are used to control the vertical motion and pitching of the aircraft. Differential collective and differential longitudinal cyclic controls rolling and yawing. In airplane mode, the tiltrotor uses the conventional aircraft controls: the elevator, ailerons, and rudder. A switching scheme is defined to change between the two different control modes based on the nacelle angle. Figure 3 shows a visualisation of the tiltrotor FLIGHTLAB model

NLR's GSP (Ref. 22) is used to compute the engine performance. GSP is an off-line component-based modelling environment for gas turbines. Both steady-state and transient simulation of any kind of gas turbine configuration can be performed by establishing a specific arrangement of engine component. The CO_2 emissions are modelled as a constant factor related to the engine fuel flow. NOx is modelled using reference turboshaft engine emission data using the ICAO engine database, Ref. 23. A correction model is applied to calculate NOx emissions at different power settings and ambient conditions. A neural network is then fitted to the engine data generated by GSP to provide FLIGHTLAB with fuel consumption and emission data for every mission segment.

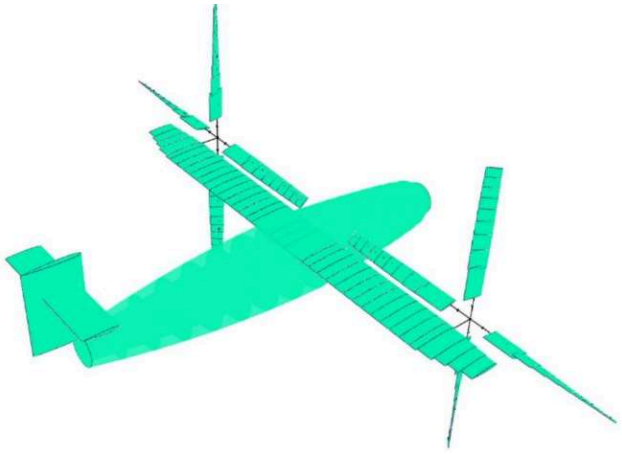

Figure 3: Large capacity tiltrotor FLIGHTLAB model representation

4.2. Simulation model compound helicopter FLC

The compound rotorcraft is modelled using the Cranfield University integrated rotorcraft simulation platform developed and validated in Ref. 11 and recently adapted to accommodate large-capacity rotorcraft and hybrid electric propulsion systems. This framework incorporates models for rotorcraft trim, unsteady rotor blade air-loads, rotor-rotor interactions, mission

analysis, engine performance, and gaseous emissions prediction.

The developed performance model approximates level 1 of Padfield's modelling hierarchy, which is suitable for performance and trade-off studies Ref. 17. A simple main rotor model which approximates Level 1/2 of Padfield's modelling hierarchy and is therefore appropriate for performance studies is employed. The main rotor model uses steady-state nonlinear blade element theory combined with the Beddoes inflow model extended by van der Wall in Ref. 24. The interaction between the two contrarotating rotors in low to moderate flight speeds is estimated using empirical models originally developed for hovering conditions and adopted for forward flight, Ref. 25. The blades are assumed to be rigid, and the flap deflections are predicted using on Padfield's model, Ref. 17. The equivalent spring stiffness for the first harmonic of blade flapping is set to 1.4 in accordance with the X2TD blades Ref. 9.

The propeller model utilises steady-state nonlinear blade element momentum theory. The fuselage and empennage are represented using look-up tables for lift and drag coefficients as a function of the angle of attack as discussed in Ref. 11. The forces and moments calculated for the rotorcraft components are resolved at the centre of gravity. For each operating condition, the rotorcraft is trimmed for a set of control angles using a Newton-Raphson root-finding algorithm, Ref. 17.

The trim module is then coupled with both an engine performance tool and a gaseous emissions prediction tool. These are then integrated within a mission analysis framework, Ref. 26.

The engine performance simulation software (*TURBOMATCH*) is employed to predict the fuel flow, engine station temperatures and pressures, and combustor inlet conditions that are used for the gaseous emissions estimations. *TURBOMATCH* robustness has been proven for several applications and engine configurations such as Ref. 27, 28. It is based on zero-dimensional analysis of the aero-thermodynamic processes occurring throughout the engine gas path, employing discrete component maps. The methodology essentially solves the mass and energy balance between the various engine components.

4.3. Mobility analysis

The EMMA (European Multi-Modal Analysis) code, developed by University of Padua in the framework of the DEPART2050 project, has been extensively used to analyze the impact of new concept aircraft and rotorcraft in the EU intermodal network. EMMA assesses the mobility benefits arising after the introduction of a new aircraft network inside the current intermodal transport network. It is additionally capable of minimizing overall travel time by determining the optimal intermodal transport combination for a given location pair. As shown in Figure 4, the model operates by integrating:

- A geography module, containing the network locations, whose nodes coincide with the most important cities of each NUTS 3 administrative region in Europe;
- Travel time matrices related to the different transport modes: car, train, airplane, and new FRCs;
- A flight route model, used to build the new aircraft network, introducing new FLC and FLT routes.

Additional details related to the EMMA model can be found in Ref. 30.

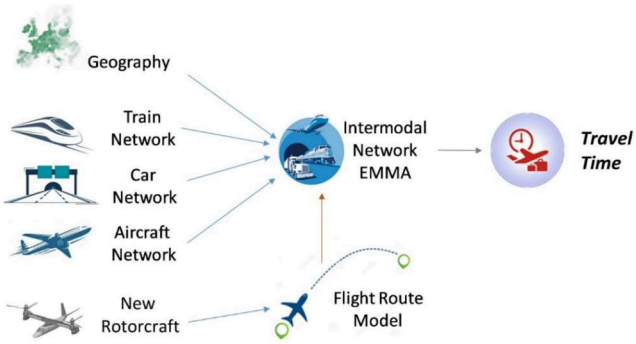

Figure 4: EMMA model structure

To understand the benefits enabled by both the large FLC and FLT concepts for passenger transport at a network level, it is necessary to identify a network optimization parameter and choose the new routes. The employed methodology can be summarized as:

- Calculation of the performance parameters related to the baseline network, considering car, train, and airplane modes.
- Choice of the network optimization parameter: in the current case population reached in less than 4 hours (PR4) for both the FLC and FLT is selected.

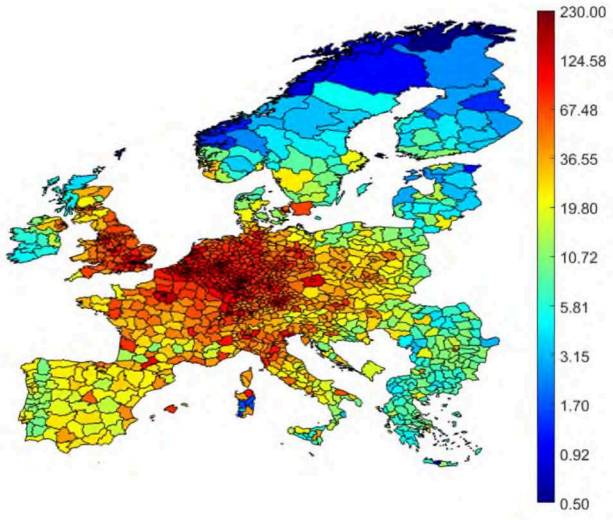

Figure 5: PR4 (in millions) for each NUTS 3 region of the baseline network

- Choice of the number of new routes composing the new aircraft network, selected among the best performing routes with respect to the optimization parameter chosen. These routes are then added to the baseline network to build the improved network.
- Calculation of the intermodal travel times and performance parameters of the improved network and compare them with the baseline network.

Mapping the PR4 level across Europe for the current baseline network (Figure 5) highlights several key aspects. For this map, each NUTS 3 region (which is a level 3 administrative division of the EU territory) is assigned a PR4 value calculated as the total population in regions that can be reached within the 4-hour travel time limit. This method means that highly populated regions, for example as the Île-de-France area, score highly.

Additionally, geographical proximity has a strong influence. This is most clearly demonstrated by the relatively low score for the Catalan region of Spain compared to the Côte-d'Azur region of France, where both regions have similar population densities. Further, large cities and NUTS 3 regions in central Europe are generally well connected to airports and are surrounded by regions with high population densities. This means that large populations are accessible with small increments in travel time. Finally, the peripheral and remote regions of Europe return low scores due to both low population densities and the time required to reach central transport hubs. These include Scandinavian regions close to the Arctic Circle, some Baltic regions, and isolated islands.

The best performing regions in Central Europe present values of PR4 between 100 and 230 million people, which for the selected countries account between 20% and 45% of the total European population of slightly more than 500 million. However, the average PR4 value for Europe is far lower, being approximately 58.7 million. The results for the FLC and FLT are presented in Chapter 5.2.

4.4. Mission analysis experiment

Four different mission scenarios have been chosen to study the performance, environmental impact, and mobility of the large FRCs. Two types of mission categories are selected:

Routes that can be operated by both VTOL & regional aircraft, which are suitable for performance comparisons with the ATR 72-600:

- London - Paris: two big metropolitan cities with high airport access times. The FLC or FLT rotorcraft would depart from London Battersea airport (ICAO: EGLW) and arrive at Issy-les-Moulineaux heliport (ICAO: LFPI). The ATR 72-600 departs from London Luton airport (ICAO: EGGW) and arrives at Paris Charles de Gaulle (ICAO: LFPG) airport.
- Amsterdam - Strasbourg: two important but smaller cities that have lower airport access times. The rotorcraft takes off from Amsterdam heliport (ICAO: EHHA) and lands at Strasbourg Neuhof small airport (ICAO: LFGC). The ATR 72-600 takes off from Amsterdam Schipol airport (ICAO: EHAM) and lands at Strasbourg Entzheim (ICAO: LFST) airport.

Routes that can be operated by VTOL only, which for airport or orographic reasons cannot be operated by the reference regional aircraft:

- Milan - Cortina: an interesting route as for the Milan Cortina 2026 Olympic Games a VTOL taxi connection is expected between the current railway yard near Porta Romana, where the Olympic village will be built, and Cortina Fiames airport (ICAO: LIDI). The route cannot be operated by a regional aircraft for both orographic reasons and size of the arrival airport.
- Berlin - Davos: a route connecting the German capital to the venue of the World Economic Forum (WEF). Both FRC aircraft depart from Berlin

Tempelhof airport (previously ICAO: EDDI), which is near the city centre, and land at the WEF Helipad in Davos. The route cannot be operated by a regional aircraft because of the absence of an airport near Davos: the nearest airport is Zurich airport, located more than 150 km and 2 hours away (by car) from Davos.

The set of missions has been chosen to cover a range of flown distances and city dimensions. The first of these is important to understand variations in performance and environmental impact, while the second considers mobility impact. Where possible, ICAO designations for airports and heliports are provided for clarity.

5. RESULTS AND DISCUSSION

5.1. Mission performance results

The performance of all three aircraft over the 500NM design mission is compared in Table 4 and Figure 6. Note that the design mission is defined with a take-off and landing segment at 5000 ft. Each aircraft flies at its (sub) optimum cruise speed and altitude. Onboard are 70 passengers with luggage, weighing 105 kg each. As observed from the Figure 6, the ATR 72-600 reference aircraft shows the expected power peak at take-off and the associated high fuel flow. During the climb phase, the power required, and fuel flow decreased until cruise flight is reached. For the ATR 72-600, the power required at the start of cruise is 52% of the max take-off power for this mission. The compound helicopter take-off phase is defined as hovering flight, with the associated high power and fuel flow. The power and fuel flow increase during climb. In cruise, the power required is 120% of the take-off hover power. The tiltrotor has the highest take-off hover power. When the tiltrotor picks up speed during the climb phase, the required power and fuel flow rapidly drop. At the start of the cruise phase, the tiltrotor power required is 54% of its take-off hover power.

Over the same 500 NM design mission, the tiltrotor completes the mission 27 minutes faster when compared to the ATR 72-600. For the performance comparison of the design mission, both aircraft start and land at the same airport. Mobility benefits coming from the ability of the tiltrotor to land at smaller airports or heliports are considered in the mobility analysis results in the next section. The mission time advantage of the tiltrotor comes from the shorter time until take-off and the higher cruise speed. The time savings of the tiltrotor comes at a cost, it consumes 26% more fuel, produces 126% more CO_2 and 24% more NOx when compared to the ATR72-600.

The coaxial compound helicopter is found to finish the 500NM mission 3 minutes faster than the ATR 72-600. The FLC has a lower cruise speed but obtains its time savings from the shorter time until take-off and after landing. The FLC consumes 206% more fuel, produces 206% more CO_2 and 278% more NOx when compared to the ATR72-600.

Table 4: Design mission performance comparison

Parameter	ATR72	FLC	FLT
Payload [kg]	7350	7350	7350
Range [NM]	500	500	500
Cruise altitude [ft]	19 000	10 000	25 000
Cruise TAS [kts]	247	214	300
Block fuel [kg]	1309.3	4004.8	2964.7
CO_2 [kg]	4163.6	12735.3	9439.6
NO_x [kg]	14.9	56.4	18.5
Mission time[min]	154.8	151.5	127.9
Norm. fuel [kg/pax/km]	0.0202	0.0618	0.0457
Norm. CO_2 [kg/pax/km]	0.0642	0.1965	0.1456
Norm. NO_x [kg/pax/km]	2.300e-4	8.701e-4	2.856e-4
Norm. time [min/km]	0.1672	0.1636	0.1382

Mission performance is also studied over the shorter 252 NM mission Amsterdam-Strasbourg. The definition of the mission is presented in Section 4.4, results are presented in Table 5 and Figure 7. Over this shorter mission, the time savings of travelling by tiltrotor compared to the ATR 72-600 reduced to 11 minutes. The FLT is found to use 149% more fuel, generated 149% more CO_2 and 33% more NOx when compared with the ATR 72-600. The FLC also shows a flight time saving of 10 minutes. When compared to the ATR 72-600, the FLC uses 179% more fuel, generates 179% CO_2 and 253% NOx. The non-dimensional mission performance parameters are compared between the longer 500 NM design mission and the shorter 252 NM Amsterdam – Strasburg mission for the different aircraft configurations. The ATR-600 uses 12% more fuel and CO_2 and 8% more NOx

per passenger per kilometre flying the 252 NM mission when compared to the 500 NM design mission.

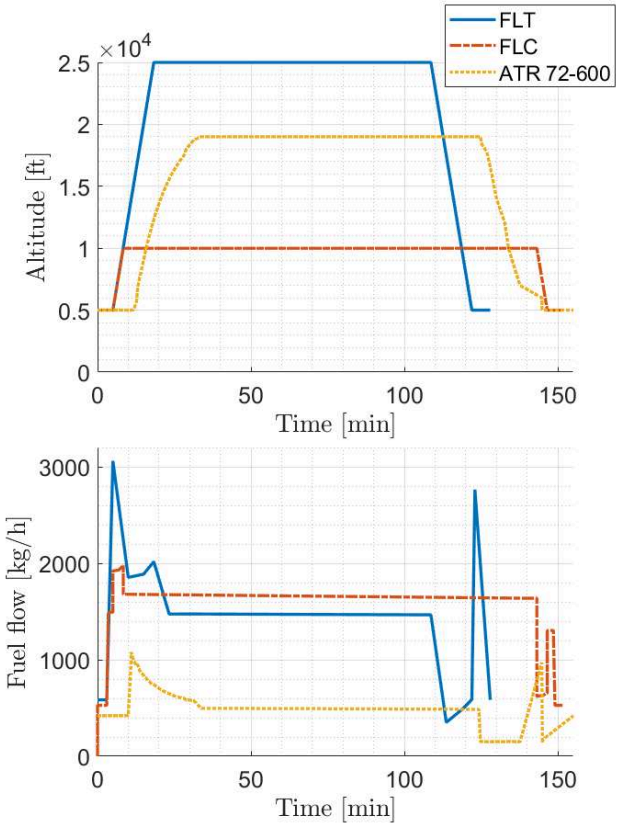

Figure 6: Design mission performance comparison of altitude (top) and fuel flow rate (bottom) against time

Table 5: Amsterdam-Strasbourg mission performance comparison

Parameter	ATR72	FLC	FLT
Payload [kg]	7350	7350	7350
Range [NM]	253	252	252
Cruise altitude [ft]	19 000	10 000	25 000
Cruise TAS [kts]	247	214	300
Block fuel [kg]	738.5	2060.8	1836.2
CO2 [kg]	2348.4	6553.4	5846.4
NOx [kg]	8.1	28.6	10.8
Mission time [min]	93.6	83.2	83.1
Norm. fuel [kg/pax/km]	0.0225	0.0630	0.0562
Norm. CO2 [kg/pax/km]	0.0717	0.2005	0.1788
Norm. NOx [kg/pax/km]	2.478e-4	8.749e-4	3.292e-4
Norm. time [min/km]	0.2000	0.1782	0.1780

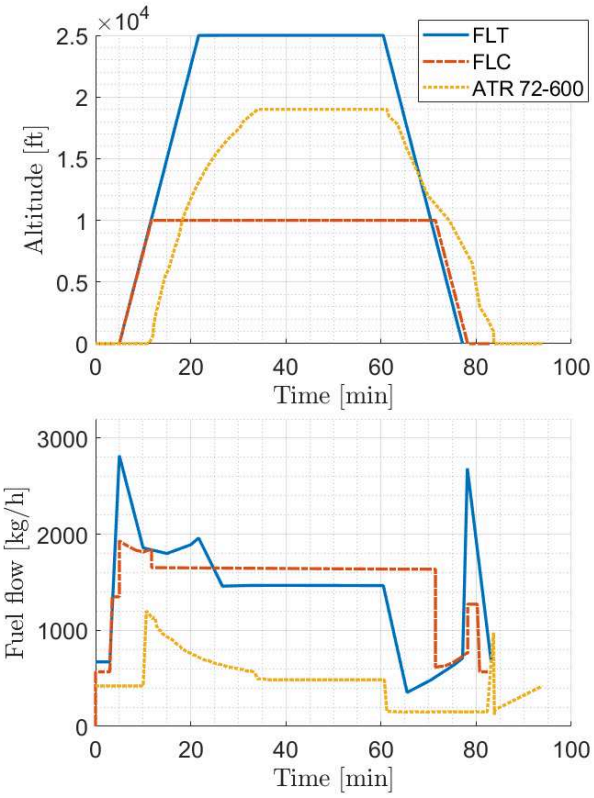

Figure 7: Amsterdam - Strasbourg mission performance comparison of altitude (top) and fuel flow rate (bottom) against time

The FLT uses 23% more fuel and CO_2 and 15% more NOx per passenger per kilometre flying the shorter mission when compared to the design mission. The FLC uses 8.9% more normalised fuel and CO_2 and 0.5% more NOx when flying the shorter mission in comparison to the design mission.

As per the specified design mission, no range credit is allocated for the descent phase of the flight due to potential constraints related to the traffic management approach route. Distinct airport or heliport approach procedures across various configurations may affect travel time and emissions, but these factors have not been considered in this analysis.

5.2. Mobility analysis results: FLC

The calculation of the total travel time (door-to-door) for four off-design missions has been carried out comparing public transport mode, car mode and traditional aviation to understand the potential time savings achievable with the new rotorcraft. It is important to note that the origins and destinations of the four trips are inside the city centre: for the London-Paris trip, the starting point has been chosen in Piccadilly Circus, whereas the arrival point is in Place de la

Concorde; for the Amsterdam-Strasbourg trip, the starting point has been chosen at the European Medicine Agency premises, whereas the arrival point is at the EU Parliament; for the Milan-Cortina and Belin-Davos routes the starting point and arrival point coincide with the origin/destination heliports, which are really close to the city centres. The sum of the travel time for each mode, including the relevant connection and waiting times (visible in Table 6), provides the total travel time for a mission. The time to reach the train station, airport and heliport has also been included assuming car mode.

Table 6: Waiting and connection times assumed in the EMMA model

Node type	Waiting time (minutes)		
	Pre-departure	Connection	Post-arrival
Airport	60	45	30
Heliport	20	25	10
Train Station	15	15	10

Two different FLC cruise speeds (235 kts and 195 kts) have been analysed, to understand the sensitivity of this parameter to the total time saving; it is clear that the time saving will come at a cost: increased fuel consumption and emissions.

As illustrated in Figure 8, in all the mission simulations the FLC rotorcraft always provides a total travel time benefit when compared to all the other means of transport. In particular, the following considerations can be drawn up:

• **Amsterdam-Strasbourg**: the FLC presents time savings of 27.5% in the low cruise speed case and 32.4% in the high speed case with respect to the second-best mode (airplane). Airport and heliport access times are similar for both Amsterdam and Strasbourg and FLC flight time is slightly higher than the ATR72. The reduction in travel time is thus due only to a lower waiting time at the heliport assumed in the model. This assumption seems reasonable until future heliports/vertiports become busy.

• **London-Paris**: the FLC scores high travel time savings in both the low cruise speed (-37.3%) and high cruise speed (-40.3%) case. The reduction in travel time is due to both reduced heliport access time (London and Paris heliports are much closer to the city centre than their airports) and also heliport waiting time. It is worth noting that the second-best transport mode is not the airplane (ATR72), but the public transport (train): in fact, the railway connection is faster than the air connection for this trip.

• **Berlin-Davos**: this is the longest route which has been simulated, and it cannot be operated by an ATR72, due to the absence of an airport in Davos. However, the airplane mode has been added assuming a flight from Berlin airport to Zurich airport, which, as said before, is more than 150 km away from Davos. Due to the long distance, the airplane mode is the best among the baseline modes and becomes the reference benchmark for the FLC time saving: a considerable reduction of 55.7% is observed in the low cruise speed case and 60.3% in the high speed case. The travel time reduction is achieved thanks to the avoidance of a 2h car travel from Zurich to Davos, coupled with a 1h reduction in airport waiting time.

• **Milan-Cortina**: this is the smallest route which has been simulated, and in this case there is no general aviation option that makes sense to compare with: the FLC has been compared only to car and public transport. The FLC scores the highest travel time reductions for this mission, with a 65.8% (low cruise speed) and 67.6% (high cruise speed) decrease in travel time with respect to the car mode. This mission underlines the advantages of using VTOLs to connect cities which may be not so far away from each other but are divided by natural barriers (in this case mountain ranges).

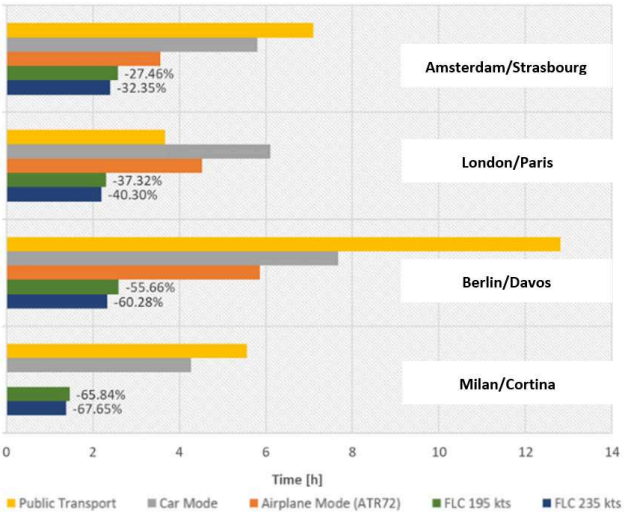

Figure 8: Travel time comparison between FLC at 2 different design cruise speeds and other means of transport for the Passenger Transport Missions.

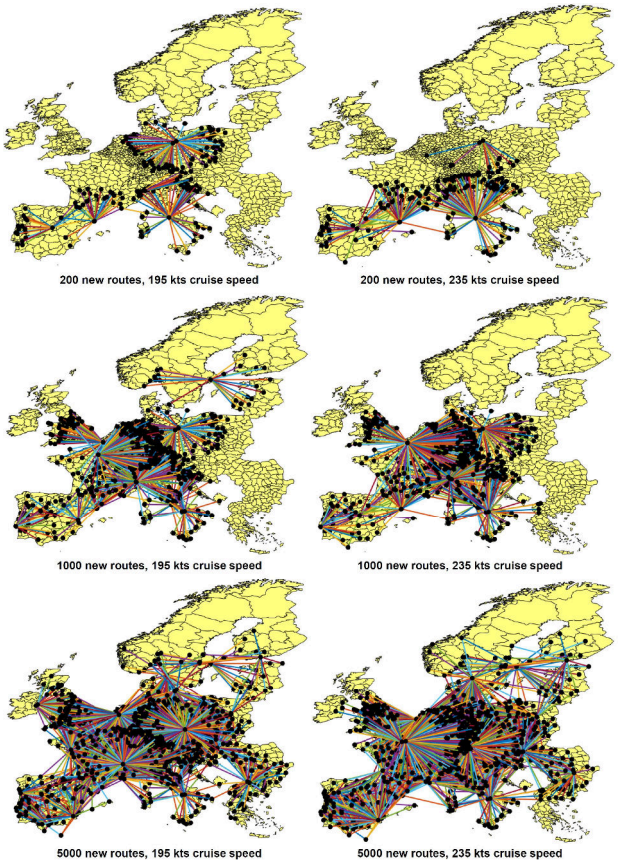

Figure 9: New optimal FLC routes chosen to maximize PR4 as a function of cruise design speed and number of new routes.

In addition, a sensitivity analysis has been carried out to evaluate the impact of the FLC on PR4, as a function of two important parameters: cruise design speed and number of new routes. The first is a rotorcraft design parameter, the second is a measure of the adoption of the new technology inside the EU. From previous studies, these two are among the parameters that have the highest mobility impact.

Since a VTOL aircraft can operate even in the absence of a runway, the whole set of European airports (from very small to big) and heliports has been used to build the new FLC network. Starting from all the possible airport combinations, the FLC maximum range, which is chosen by design to be 500 NM, will define a threshold: all the connections with a flight distance higher than this value will be discarded. More than 7000 airports have been considered in the calculations: this means that even filtering all the connections with a maximum range will lead to hundreds of thousands of routes. From a practical point of view, only a small fraction of these potential airport combinations will be operated by the FLC in the future.

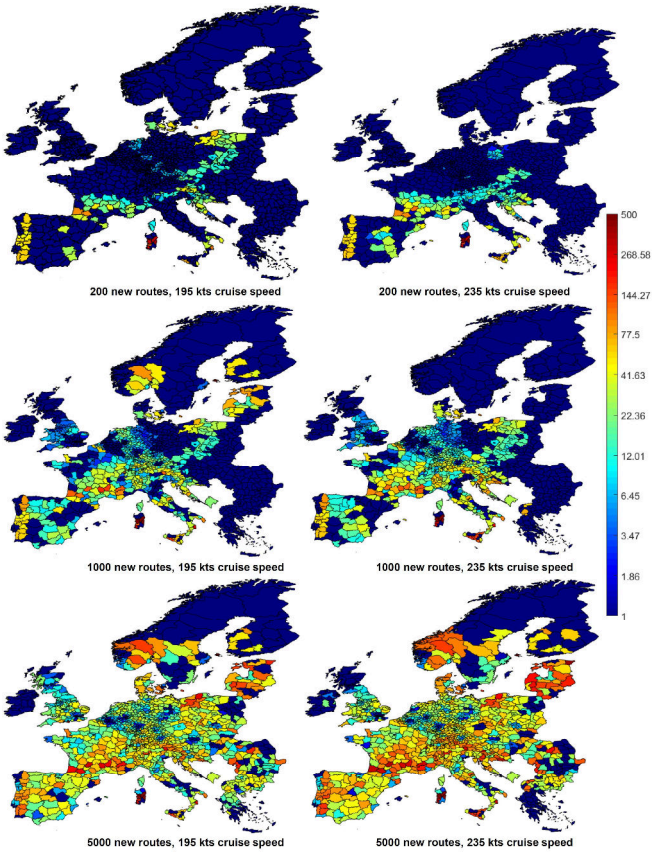

Figure 10: Increment in PR4 [%] due to the FLC routes distributed among EU NUTS3 regions as a function of cruise design speed and number of new routes.

For this reason, only the best performing routes will be used to build the FLC network.

The performance parameter chosen to identify the best new routes is, as discussed before, PR4. The EMMA code ranks all the feasible new routes based on the increase of overall European PR4 and adds to the baseline network the ones having the highest beneficial impact.

Six different European scenarios have been simulated:

# of new routes	Cruise Speed (kt)
200	195
200	235
1000	195
1000	235
5000	195
5000	235

The newly built FLC networks for each of the six abovementioned scenarios are visible in Figure 9. The percentage increase in PR4 for each NUTS 3

region, achieved with the introduction of the new routes can be observed in Figure 10. Observing these figures, some interesting considerations can be made:

1. Changing the cruise speed has an impact on the choice of the optimal routes, because the increase in cruise speed (40 kts) is able to rise the number of trips that can be achieved in less than 4 hours. If the new trips put in contact a higher amount of population, the ranking of the best routes changes. This is why in Figure 9 different routes are chosen by the algorithm on the left-hand side (195 kts) and on the right-hand side (235 kts).
2. To optimize PR4 the algorithm is favouring spoke-hub connections, which help to achieve a higher connectivity between a big city/metropolis and its peripheral regions. This boosts the PR4 values of the peripheral regions, because a quick access to a large international airport permits to reach other big European cities in less than 4 hours.
3. The maximum PR4 gains are encountered in those regions which are directly connected to a metropolis with a new FLC route. The big cities instead, do not experience big percentage increases because they are already well connected with scheduled airplane routes. To improve visualization capability and facilitate the comparison between the different cases, the legend in all the figures is limited to 500% PR4 increase. However, much higher gains are possible, since deep red regions correspond to increments equal or higher than 500%. Taking a poorly connected region as example, the ITG2A region of Sardinia, the following is found: for the 195 kts FLC in the 200 new routes case the maximum PR4 gain is about 390% (654% for 235 kts); in the 1000 new routes case the increase is equal to 660% (983% for 235 kts); in the 5000 new routes the gain reaches 784% (1270% for 235 kts).
4. The number of new routes highly affects the PR4 increase: this is clearly visible from Figure 10. In order to understand the impact at a network level, a new global mobility performance parameter is introduced: average PR4. It is calculated as the average of the PR4 values among all the 1396 NUTS 3 regions. It represents therefore the average number of people reachable in less than 4h starting from a generic location in the EU. The average PR4 for the EU is approximately 58.7 million people.

Looking at a global network parameter, the percentage increase in average PR4 as a function of FLC cruise speed and the number of new FLC routes is visible in Figure 11. As a remainder, the average PR4 value for the entire European continent is approximately 58.7 million. With only 200 new routes, the impact on average PR4 is really modest (around 1% increase); with 1000 new routes, the gains are higher, but less than 10%; with 5000 new routes, the gains are between 20% and 30%. The cruise speed impact increases with the number of new routes, both in absolute and relative terms.

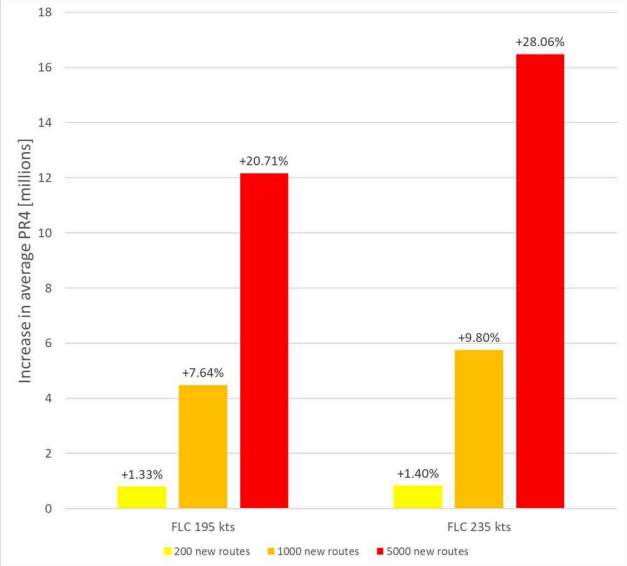

Figure 11: Increase in average PR4 for the FLT at different design cruise speeds and number of routes.

5.3. Mobility analysis results: FLT

The calculation of the total travel time (door-to-door) for the four missions previously defined has been carried out in the same way as described for the FLC rotorcraft (section 5.2). The same considerations on the missions apply. From a mobility standpoint, the main difference with respect to the large compound rotorcraft is the increased cruise speed: two different FLT cruise speeds (270 kts and 300 kts) have been analyzed, to understand the sensitivity of this design parameter on the total time saving. There is no other major mobility difference, since the maximum range is the same for both the FLC and FLT, and the two aircraft can operate on the same heliports/small airports.

As illustrated in Figure 12, in all the off-design mission simulations the FLT aircraft always gets a large reduction in total travel time, compared to all the other means of transport. In particular, the following considerations can be drawn up:

• **Amsterdam-Strasbourg**: the FLT presents time savings of 35.4% in the low cruise speed case and 36.9% in the high speed case with respect to the second best mode (airplane). In the 270 kts case, the flight time is very similar to the ATR72, while in the 300 kts the flight time is slightly reduced (approximately -4%). The reduction in travel time is therefore mainly attributable to the lower waiting time at the heliport.

• **London-Paris**: the FLT scores high travel time savings in both the low cruise speed (-42.2%) and high cruise speed (-42.9%) case with respect to the train mode. The difference between low cruise speed and high cruise speed cases is lower with respect to the previous mission because of the reduced distance. The reduction in travel time is mainly due to reduced heliport access and waiting times, and very slightly due to reduced flight time.

• **Berlin-Davos**: a considerable reduction of 63.2% for the FLT is observed in the low cruise speed case and 64.8% in the high speed case with respect to the traditional air transport. The travel time reduction, as for the FLC, is achieved mainly thanks to the avoidance of a 2h car travel from Zurich to Davos, coupled with a 1h reduction in airport waiting time.

• **Milan-Cortina**: the FLT scores the highest travel time reductions for this mission, with a 68.8% (low cruise speed) and 69.0% (high cruise speed) decrease in travel time with respect to the car mode. The difference between 270 kts and 300 kts cases is the lowest with respect to the previous missions because it's the mission characterized by the lowest travelled distance. As seen also for the FLC, this mission underlines the advantages of using VTOLs to connect cities divided by natural barriers.

Moreover, a sensitivity analysis has been carried out to evaluate the impact of the FLT on PR4, as a function of cruise design speed and number of routes, as done also for the FLC rotorcraft in section 5.2.

The performance parameter chosen to identify the best new routes is again PR4. The EMMA code ranks all the feasible new routes based on the increase of overall European PR4 and adds to the baseline network the ones having the highest beneficial impact.

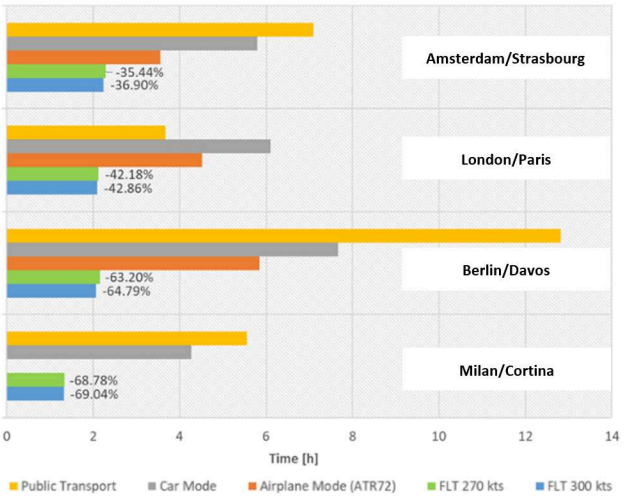

Figure 12: Travel time comparison between FLT at 2 different design cruise speeds and other means of transport for the Passenger Transport Missions.

Six different European scenarios have been simulated:

# of new routes	Cruise Speed (kt)
200	270
200	300
1000	270
1000	300
5000	270
5000	300

The newly built FLT networks for each of the six abovementioned scenarios are visible in Figure 13. The percentage increase in PR4 for each NUTS 3 region, achieved with the introduction of the new routes can be observed in Figure 14. Observing these figures, some interesting considerations can be made:

1. Changing the cruise speed has a mild impact on the choice of the optimal routes, with respect to the FLC previous results. This is due to two reasons: the reduced increase in cruise speed both in absolute terms (30 kts with respect to 40 kts) and relative percentage terms (11.1% against 20.5%). In fact, in Figure 14 the difference between the chosen routes on the left-hand side (270 kts) and on the right-hand side (300 kts) is much lower with respect to Figure 10.
2. As seen before, to optimize PR4 the algorithm is favouring spoke-hub connections, which help to achieve a higher connectivity between a big city/metropolis and its peripheral regions. This boosts the PR4 values of the peripheral regions,

which are granted a quick access to a large international airport.

The maximum PR4 gains are encountered in those regions which are directly connected to a metropolis with a new FLT route. The big cities instead, do not experience big percentage increases because they are already well connected with scheduled airplane routes. The legend in the figures is limited to 500% PR4 increase, but even higher gains are possible. Taking a poorly connected region as example, the ITG2A region of Sardinia, the following is found: for the 270 kts FLT in the 200 new routes case the maximum PR4 gain is about 335% (same for 300 kts); in the 1000 new routes case the increase is equal to 1463% (1008% for 300 kts); in the 5000 new routes the gain reaches 1951% (2161% for 300 kts). The differences in PR4 between the two different cruise speeds are lower with respect to the FLC case, mainly due to the reasons discussed in point 1. It even happens that increasing the speed may decrease the PR4 value of a specific region.

It may seem counterintuitive, but the explanation is simple: the increase in speed has favored the choice of slightly different routes, decreasing the number of routes connecting that specific region. The average PR4 value in the EU will increase, but regions that have been cut out due to the choice of different routes will have a reduced mobility benefit. The number of new routes highly affects the PR4 increase: this is clearly visible from Figure 14. To understand the impact at a network level, the percentage increase in average PR4 is plotted in Figure 15. With only 200 new routes, the impact on average PR4 is very low (around 1.5% increase); with 1000 new routes, the gains are higher, around 10%; with 5000 new routes, the gains are between 30% and 40%. The cruise speed impact increases with the number of new routes, both in absolute and relative terms, as seen also for the FLC aircraft.

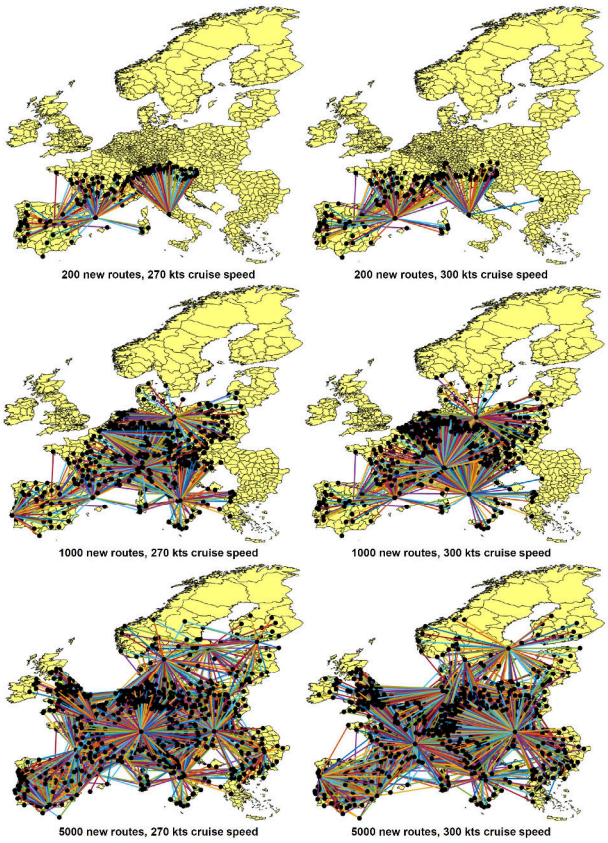

Figure 13: New optimal FLT routes chosen to maximize PR4 as a function of cruise design speed and number of new routes.

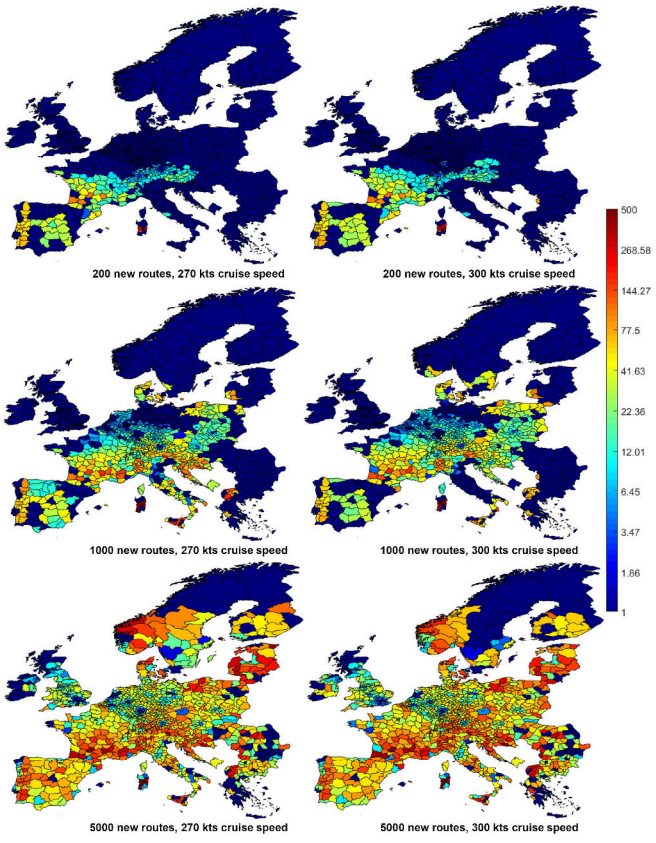

Figure 14: Increment in PR4 [%] due to the FLT routes distributed among EU NUTS3 regions as a function of cruise design speed and number of new routes.

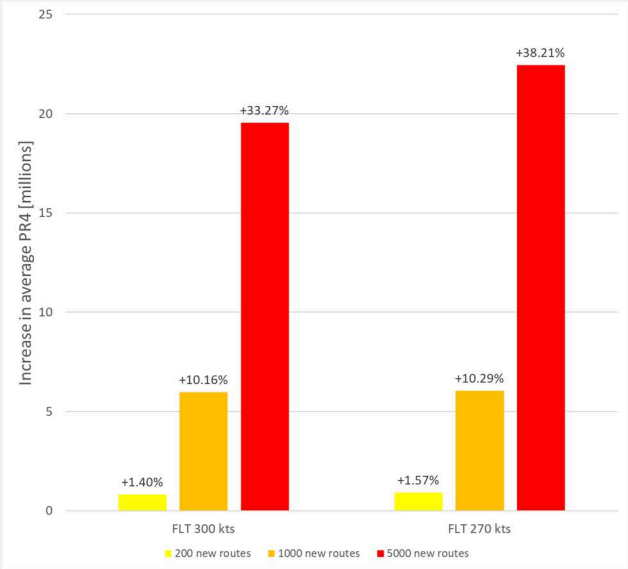

Figure 15: Increase in average PR4 for the FLT at 2 different design speeds. The impact on average PR4 is evaluated as a function of the number of new routes.

6. CONCLUSIONS

The increasing need for efficient transportation drives the exploration of Fast Rotorcraft Concepts (FRCs) to alleviate congestion and improve mobility. Project FASTRIP2050, a part of European Clean Sky 2, investigates large capacity tiltrotor and compound rotorcraft performance, mobility, and environmental impact. FRCs could shift short-haul traffic to rotorcraft, reducing airport congestion and offering new intercity and commuter connections. Mission performance results were compared against the ATR 72-600 reference aircraft. Mobility analysis benefits were compared against other modes of transport.

A 500 NM design mission was defined to size both FRC concepts, the Fast Large Tiltrotor (FLT) and the Fast Large Compound (FLC) coaxial rotorcraft. The design mission range is based on operating data of the ATR72-600 reference aircraft and the volume of flights in this range segment, 40% of global departures. The ATR 72-600 and FLC flight and engine performance are computed using Cranfield University integrated rotorcraft simulation platform in combination with the university's engine performance simulation software (TURBOMATCH). The FLT is simulated by the Royal Netherlands Aerospace Centre using FLIGHTLAB and their in-house gas turbine simulation tool GSP.

1. In this paper, mission performance results were assessed over the 500 NM design mission and the 252 NM Amsterdam–Strasburg mission. Mission time is reduced by the use of FRCs, with the FLT providing the largest benefit for all missions. The FLC suffers time penalties as mission distance increases due the low cruise speed relative to both FLT and ATR.
2. The FLT shows the highest power required peak during its take-off phase which is defined as hovering flight. When the tiltrotor picks up forward speed to climb, the power required decreases until cruise is reached. The FLC coaxial rotorcraft has a lower hover power when compared to the tiltrotor. However, for this FLC configuration, the power required in high speed cruise is higher than the hover power.
3. The environmental performance for both FRCs compared to the fixed-wing baseline does not show benefits at the current engine technology levels. In particular the high cruise power requirement of the FLC is extremely detrimental to its environmental performance.

The EMMA tool was deployed to explore the mobility impact of the two FRC aircraft when used for defined destination missions and for optimizing new routes within the intermodal transport network. The assessment parameters were PR4 (population reached in less than four hours) for the latter and mission time for the former.

4. When comparing mission time across all modes of transport for any of the selected missions, the FRC deliver significant benefits (Figure 16). EMMA reveals that while conventional air transport is generally quickest, this is not always true for well-connected cities such as London and Paris where public transport can provide a very short journey.
5. For poorly connected destinations, such as Davos which lacks an airport in proximity, the choice of conventional air travel relies heavily on the support of other modes to complete the journey. The FRCs, however, could deliver passengers much closer to their destination without need for such connections and the inherent risk of delay.
6. Finally, the impact of cruise speed and number of additional routes was evaluated for both FRC. The highest cruise speed for the FLT delivers the maximum benefits, as would be expected, especially when compounded by the highest number of new routes. This should be extended to assess

the impact of FRC in regions outside of Europe where the underlying transport network may be less well developed, thereby maximizing the impact of FRCs.

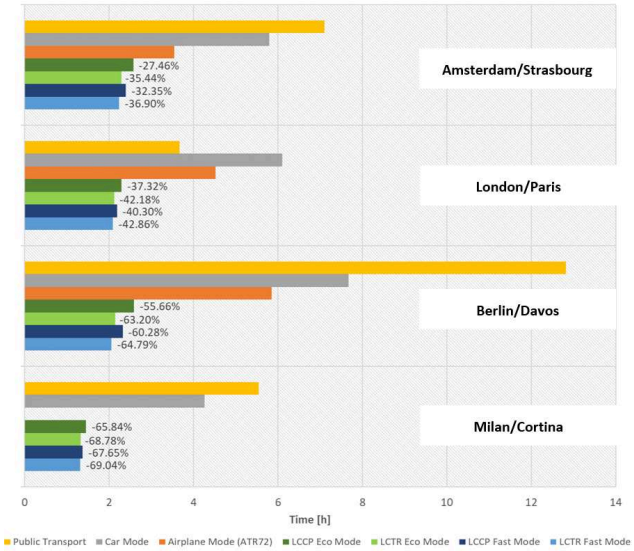

Figure 16: Summary of the overall passenger transport mission results.

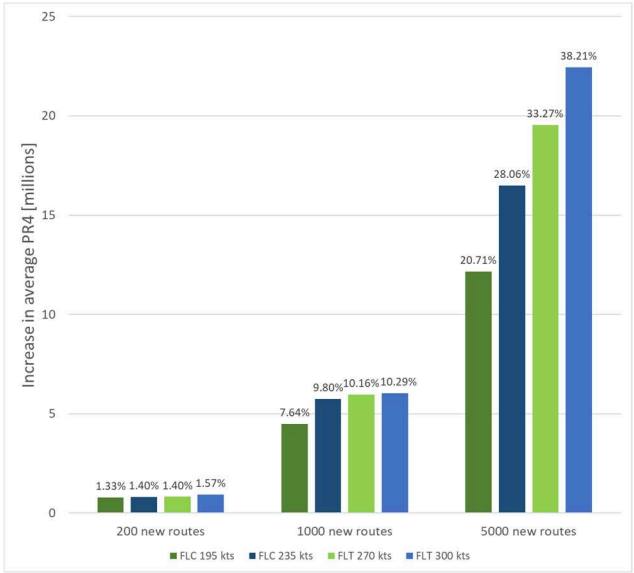

Figure 17: Effect of cruise speed and number of new routes on PR4.

7. FUTURE WORK

As part of FASTRIP2050, the authors will be looking at the possibility of reducing emissions of CO_2 and NOx by using electric motors that provide power to either assist or fully take over from the gas turbine. Based on fuel flows as shown in Figure 4, three options could be considered:

1. the electric engine is active for a short time during the peak in fuel flow (take-off and landing)

2. the electric engine is active for a long duration during cruise

3. the electric engine is active during all flight mission phases.

Flying fully on electric power would not be feasible without significantly affecting range and payload with current battery technology. The analysis will, therefore, focus on hybrid propulsion in which the electric engine provides power to assist the gas turbine. Furthermore, current battery technologies have a trade-off in their performance: the higher the specific power, the lower the specific energy and vice versa Ref. 31. A battery with high specific power is advantageous for peak power situations (hover, OEI), whereas high specific energy is desired for long durations at lower power levels (cruise). Therefore, the first step in reducing emissions will be to look at which flight phase would provide the largest reduction were it to be powered partially with electric power. The option of flying with hybrid power during the entire flight will not be considered since it would require a battery that is high both in specific power and energy or two batteries with one high on specific power and the other high on specific energy. The latter would complicate further the weight estimation of the entire electric system and will thus, at least initially, not be considered in future work.

To simulate a mission with hybrid propulsion, the tool described in Section 4.1 needs to be expanded to account for electric power and the electric system weight. FLIGHTLAB provides the total necessary power for trim at every mission point. A percentage of that total power is now assumed to be provided by the electric propulsion system. This power per mission point is fed into MASS, a tool developed at NLR to estimate the weight of the complete electrical power system. MASS takes as inputs the power required provided by FLIGHTLAB and assumptions on the electrical system efficiencies and specific power and energy of the batteries. It then calculates the weight of the battery and other system components necessary to fly the mission. The outputs are the state of charge of the battery per mission point as well as the weights of the different electric system components, including the battery itself, the electric motor, the inverter, the cabling, and the cooling system. The payload then needs to be reduced by the total mass of the electric power system since the MTOW is chosen

to stay constant. If the weight of the electric system is larger than the available payload mass, the percentage of electric power needs to be reduced until it becomes smaller. A new FLIGHTLAB iteration is then needed. Electric power changes fuel consumption, which affects the weight of the rotorcraft and thus the power required and therefore the electric power weight too. Iterations will be necessary until the weights converge to a stable value.

Using electric power will reduce emissions per flight but also reduces the number of passengers by significant amounts with current battery technology. Therefore, use of electric power is expected to increase emissions per passenger with current battery technology. Future work will investigate what are the necessary specific power and energy improvements needed to start obtaining emission reductions per passenger.

The FLC presents as a particular challenge for electrification due to the peak power demand arising not during hover phase but during the forward flight phase (Figure 2). This precludes the use in situation 1 (take-off and landing deployment). Thus, the specific power becomes less critical than the specific energy for this concept and situation 2 may become feasible when battery technology matures. In this light, alternative fuels become of interest and the authors plan to assess the use of hydrogen as a fuel.

It is also planned that future concept engines will also be assessed under FASTRIP. These will incorporate high efficiency compressor stages with higher overall pressure ratios and lean combustion technologies to address the relatively poor environmental performance of the FRCs. In combination with the novel propulsion concepts above, it is envisaged that this will reduce the gap between FRCs and fixed-wing regional aircraft.

Regarding mobility, the studies performed at the European level will be extended to additional extra-EU regions, in order to understand the impact of the introduction of FRCs in intermodal transport networks which are less developed and lower connected.

Author contact:

Laurent Declerck laurent.declerck@nlr.nl

Marc Cruellas Bordes marc.cruellas.bordes@nlr.nl

Chana Saias chana-anna.saias@cranfield.ac.uk

Devaiah Nalianda devaiah.nalianda@cranfield.ac.uk

Deneys Schreiner b.deneys.j.schreiner@cranfield.ac.uk

Gianluigi A. Misté gianluigi.miste@unipd.it

Andrea Dal Monte andrea.dalmonte@unipd.it

Ernesto Benini ernesto.benini@unipd.it

8. ACKNOWLEDGMENTS

This European Union (EU) project's achievements owe gratitude to our partners. The FASTRIP2050 collaboration, exploring advanced fast rotorcraft, was supported by the Clean Sky 2 Joint Undertaking. Thanks to Royal Netherlands Aerospace Centre, ANOTEC, University of Padua, and Cranfield University for their vital roles in shaping this research.

This project has received funding from the Clean Sky 2 Joint Undertaking (JU) under grant agreement No 101007453. The JU receives support from the European Union's Horizon 2020 research and innovation programme and the Clean Sky 2 JU members other than the Union.

9. REFERENCES

1. Johnson, J., Stouffer, V., Long, D. and Gribko, J., "Evaluation of the National Throughput Benefits of the Civil Tiltrotor", NASA CR 2001-211055, September 2021
2. U.S. Congress, Office of Technology Assessment, "New Ways: Tiltrotor Aircraft & Magnetically Levitated Vehicles," OTA-SET-507, Oct. 1991, U.S. Government Printing Office, Washington, DC
3. Schäfer, A.W., Barrett, S.R.H., Doyme, K. et al. "Technological, economic and environmental prospects of all-electric aircraft." Nat Energy 4, 160–166 (2019). DOI: 10.1038/s41560-018-0294-x
4. Leonardo Helicopters, "Civilian Tiltrotor Aircraft AW609", leonardo.com/en/products/aw609 (accessed Jan. 2023).
5. Leonardo, "Next Generation Civil Tiltrotor NGCTR", www.leonardo.com/en/business/next-generation-civil-tiltrotor-ngctr (accessed Jan. 2023)

6. de Bruin, A.C., and Schneider, O., “Rotor-wing interaction phenomena for the ERICA tilt-wing rotorcraft configuration in the DNW-LLF wind tunnel,” 41st European Rotorcraft Forum, Munich, Sep. 2015
7. Johnson, W., Yamauchi, G.K., and Watts, M.E., “Designs and Technology Requirements for Civil Heavy Lift Rotorcraft” NASA, AHS Vertical Lift Aircraft Design Conference, 2006
8. Acree, C.W., Yeo, H., and Sinsay, J.D., “Performance Optimization of the NASA Large Civil Tiltrotor,” Ames Research Center, Aero flight dynamics Directorate, NASA/TM–2008-215359, Jun. 2008
9. Blackwell, R., and Millott, T., 2008, “Dynamics Design Characteristics of the Sikorsky X2 TechnologyTM Demonstrator Aircraft,” 64th Annual Forum of the American Helicopter Society, Montreal, Canada, Apr. 29–May 1, pp. 886–898
10. Walsh, D., Weiner, S., Arifian, K., Lawrence, T., Wilson, M., Millott, T., and Blackwell, R., 2011, “High Airspeed Testing of the Sikorsky X2 TechnologyTM Demonstrator,” 67th Annual Forum of the American Helicopter Society, Virginia Beach, VA, May 3–5, pp. 2999–3010
11. Scullion, C., Vouros, S., Goulos, I., Nalianda, D., and Pachidis, V., "Optimal Control of a Compound Rotorcraft for Engine Performance Enhancement." ASME. J. Eng. Gas Turbines Power. February 2021; 143(2): 021005. doi: 10.1115/1.4049163
12. Harendra, P.B., Joglekar, M.J., Gaffey, T.M., and R. L. Marr, “V/STOL Tilt Rotor Study - Volume V: A Mathematical Model For Real Time Flight Simulation of the Bell Model 301 Tilt Rotor Research Aircraft,” Tech. Rep. 301-099-001, Bell Helicopters, 1973
13. Yeo, H., and Johnson, W., 2009 “Optimum Design of a Compound Helicopter,” AIAA Journal of Aircraft, vol. 46, no. 4.
14. Yeo, H., 2019, “Design and Aeromechanics Investigation of Compound Helicopters,” Aerosp. Sci. Technol., 88, pp. 158–173
15. Johnson, W., Moodie, A.M., and Yeo, H., “Design and performance of lift-offset rotorcraft for short-haul missions,” Am. Helicopter Soc. Int. - Futur. Vert. Lift Aircr. Des. Conf. 2012, pp. 156–181, 2012.
16. Rotorcraft Systems Investigation,” NASA/TP–2005-213467, Dec. 2005.
17. Padfield, G.D., 2007, “Helicopter Flight Dynamics—The Theory and Application of Flying Qualities and Simulation Modelling”, Wiley, Chichester, UK
18. ATR Aircraft, “ATR 72-600 [Fact sheet].” atr-aircraft.com.www.atraircraft.com/wp-content/uploads/2020/07/Factsheets_-_ATR_72-600.pdf (Accessed Jan. 2023)
19. Hackneya, R., Nikolaidis, T., and Pellegrini, A., (2020), “A Method for Modelling Compressor Bleed in Gas Turbine Analysis Software”, Applied Thermal Engineering, Vol. 172
20. Diaz, S., Desopper, A., and Mouterde, E., “Performance Code for Take-Off and Landing Tilt-Rotor Procedures Study,” in 30th European Rotorcraft Forum, 2004
21. Saß, K., “Modelling and Optimization of Tilt-Rotor Aircraft Flight Trajectories,” MSc Thesis, Delft University of Technology, 2018
22. W. P. J. Visser and M. J. Broomhead, “GSP, a Generic Object-Oriented Gas Turbine Simulation Environment,” in Volume 1: Aircraft Engine; Marine; Turbomachinery; Microturbines and Small Turbomachinery, Munich, Germany: American Society of Mechanical Engineers, May 2000, p. V001T01A002. doi: 10.1115/2000-GT-0002
23. EASA, “ICAO Aircraft Engine Emissions Databank”, www.easa.europa.eu/en/domains/environment/icao-aircraft-engine-emissions-databank (Accessed Jun. 2023)
24. van der Wall, B.G., 2000, “The Effect of HHC on the Vortex Convection in the Wake of a Helicopter Rotor,” Aerosp. Sci. Technol., 4(5), pp. 321–336.
25. Yana, J., and Rand, O., 2012, “Performance Analysis of a Coaxial Rotor System in Hover: Three Points of View,” 28th International Congress Aeronautical Sciences, Brisbane, Australia, Sept. 23–28, Paper No. ICAS2012-2.7.4
26. DEPART2050, 2021, Quantification of CS2 benefits for world fleet scenarios in terms of environmental impacts and enhanced mobility, Deliverable 7
27. Hackneya, R., Nikolaidis, T., and Pellegrini, A., (2020), “A Method for Modelling Compressor Bleed in Gas Turbine Analysis Software”, Applied Thermal Engineering, Vol. 172.
28. Pellegrini A., Nikolaidis T., Pachidis V., Kohler S., (2017), “On the Performance Simulation of Inter-Stage Turbine Reheat”, Applied Thermal Engineering, Vol. 113.
29. Goulos, I., Ali, F., Tzanidakis, K., Pachidis, V., and D’Ippolito, R., 2014, “A Multidisciplinary Approach for the Comprehensive Assessment of Integrated Rotorcraft–Powerplant Systems at

Mission Level," ASME J. Eng. Gas Turbines Power, 137(1), p. 012603.
30. Misté, G.A., Venturelli, G., and Benini, E., "Mobility Impact Assessment of Innovative Aircraft inside the European Multimodal Transport Network", Proceedings of the AIAA Aviation Forum 2021, August 2021. doi:10.2514/6.2021-2952
31. Kühnelt, H., Mastropierro, F., Zhang, N., Toghyani, S., Krewer, U., (2023), "Are batteries fit for hybrid-electric regional aircraft?", J. Phys.: Conf. Ser. 2526 012026
32. Ashby, D., Eadie, W., Montoro, G.J., "An Investigation of the Reverse Velocity Rotor Concept and Its Application to High-Speed Rotorcraft", 2002, Biennial International Powered Lift Conference and Exhibit, doi: 10.2514/6.2002-5991

Performance, environmental, and mobility analysis of large capacity fast rotorcraft configurations for the European regional air traffic market

Declerck, Laurent

2023-09-07

Declerck L, Cruellas Bordes M, Saias CA, et al., (2023) Performance, environmental, and mobility analysis of large capacity fast rotorcraft configurations for the European regional air traffic market. In: 49th European Rotorcraft Forum (ERF49 2023), 5-7 September 2023, Bückeburg, Germany

https://publikationen.dglr.de/?id=620&tx_dglrpublications_pi1[document_id]=54801077